

# Wind pressures on low-rise hip roof buildings

Shakeel Ahmad<sup>†</sup>

*Department of Civil Engineering, Aligarh Muslim University, Aligarh, India*

Krishen Kumar<sup>‡</sup>

*Department of Civil Engineering, University of Roorkee, Roorkee, India*

*(Received October 16, 2000, Revised March 3, 2001, Accepted January 9, 2002)*

**Abstract.** Seven hip roof building models for 10°, 15°, 20°, 25°, 30°, 35° and 40° roof pitch with large overhangs of 1.1 m were tested in a wind tunnel at the university of Roorkee, India to investigate wind pressure distributions over hip roofs for various roof pitch and wind direction. The results show that the roof pitch and wind direction do significantly affect the magnitude and distribution of the roof pressures. The 40° roof pitch has been found to experience the highest peak suctions at the roof corners amongst the seven hip roofs tested. Pressures on 15°, 20° and 30° hip roofs are comparable with those reported by Xu and Reardon (1998). Meecham *et al.* (1991) for 18.4° hip roof is compatible with 15° hip roof of the present study. Holmes's works (1994) on gable roof have also been compared with the present work. Zoning for codification has also been attempted since IS875 (Part-3) does not include this information. A comparison for design value has also been made with BRE Report No. 346.

**Key words:** low-rise building; hip roof; TTU building; gable roof; pressure coefficients

---

## 1. Introduction

A high percentage of population of the world lives in the tropics, especially in the coastal regions, where advantage can be taken of the natural cooling effects of the sea breeze and trade winds. Unfortunately many of these coastal regions are also liable to be subjected to the winds generated by extreme tropical cyclones, known in some localities as 'typhoons' or 'hurricanes'.

Wind loads on low buildings have not received the attention they deserve when the large investment in such structures is considered. Unfortunately, they have an inconvenient way of reminding us of this neglect when a hurricane or tornado strikes.

It has been long recognized that roof geometry used in houses and low-rise buildings may significantly influence wind pressures on roofs due to change in flow patterns around the houses and buildings. Extensive wind tunnel studies carried out by Davenport, Surry and Stathopoulos (1978) and Holmes (1994) have led to certain important conclusions regarding the effect of roof slope upon the wind pressures on low-rise buildings with a gable roof. Several post disaster investigations on wind induced damage to building roofs reveal that hip roofs have performed better than the gable roofs during severe cyclones (Sparks, Baker, Belville and Perry 1985, Federal Emergency Management

---

<sup>†</sup> Reader

<sup>‡</sup> Professor



and 14). This shows that higher probability of suctions is for corner tap. Averaged point pressure coefficients have been calculated for various zones of the roof for angle of wind attack between 0° and 90° at an increment of 15°.

1.1. Experimental program

Experiments were carried out in an open circuit wind tunnel having a test section 15 m long, 2.1 m wide and 2.0 m high at the University of Roorkee (India).

Seven hip roof building models of a building, 14 m × 7 m in plan and having 2.9 m eave height with a large overhang of 1.1 m, were made at a geometric scale of 1:50 with roof slope varying from 10° to 40° at an increment of 5°. In consideration of the symmetry of the building, a total of 62 taps were arranged on half of the roof (Fig. 1), except for the 20° and 30° roof slopes where 124 taps were arranged on the whole roof to verify the symmetry condition. Particular attention has been paid to the total number and positions of the taps near the hip ridge, roof ridge and roof edge, from where the air flow may get separated to form a region of high velocity gradients with high local

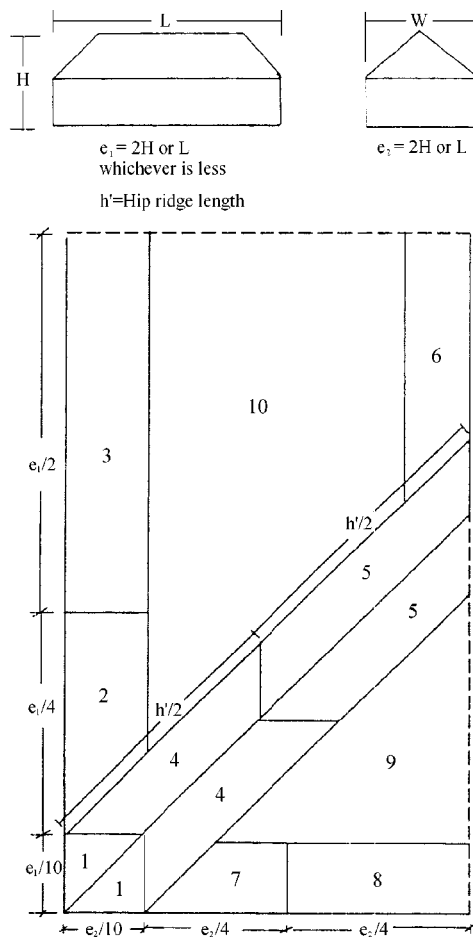


Fig. 2 Schematic diagram for different zones on hip roof building model

turbulence and vorticity. The quadrant portion of the roof has been divided into ten different zones (Fig. 2) based on the BRE Report No. 346 Nov. 1989.

The building models were fabricated using 6 mm thick ‘Perspex sheet’. Pressure taps 10mm long, 1.3 mm external diameter and 1.00 mm internal diameter of stainless steel tubing were inserted into the holes drilled in the Perspex sheet with one end of the tap flushed with the roof surface.

The tubing for measuring the surface pressures consisted of 500 mm vinyl tubes with a 40 mm restrictor placed at 400 mm from the pressure point. Pressure measurements were carried out by using Scanivalve ZOC12, a 32-port pressure scanner, having a linear response upto 100 Hz. The sampling rate was kept at 375 samples per second per channel and the duration of each run was 32 seconds (for hip roof). The total measurement of time for the almost continuous five records is about 160s. This corresponds to from 32 to 65 min in full scale depending on design wind speeds and design philosophy (AS 1170.2, 1989). Whereas duration of each run for TTU model was kept 20 seconds which is equivalent to 15 min duration on prototype.

Natural wind was developed for the 1:50 scale hip roof model to simulate the wind over open country terrain. The simulation was done on the basis of Texas Tech University (TTU) full-scale data. The velocity profile and the longitudinal turbulence intensities obtained in the tunnel are shown in Figs. 3 and 4. The mean longitudinal wind speed profile measured in the wind tunnel is in good agreement with TTU full-scale profile with a power law exponent of 0.15. The longitudinal turbulence intensity at the model eave height is 19%, which satisfies the field condition at eave height. The Small Scale Turbulence Content ( $S$ ) which is defined as  $S=[n S_u(n)/S_u^2] [S_u/U]^2 \times 10^6$  evaluated at  $n=10U/L_p$  where,  $n$  is frequency,  $S_u(n)$  is spectral density,  $S_u$  is the standard deviation of the longitudinal mean velocity ( $U$ ) and  $L_p$  is the characteristic model dimension, is found to be 85. The model eave height has been taken as the characteristic dimension. The integral scale was also evaluated at model eave height of the longitudinal wind velocity and found to be 0.45 m.

To check the reliability of the data, a 1:50 scale model of TTU building (Fig. 5) of plan dimension 13.7 m  $\times$  9.1 m with eave height 4.0 m, was fabricated and tested in the simulated flow

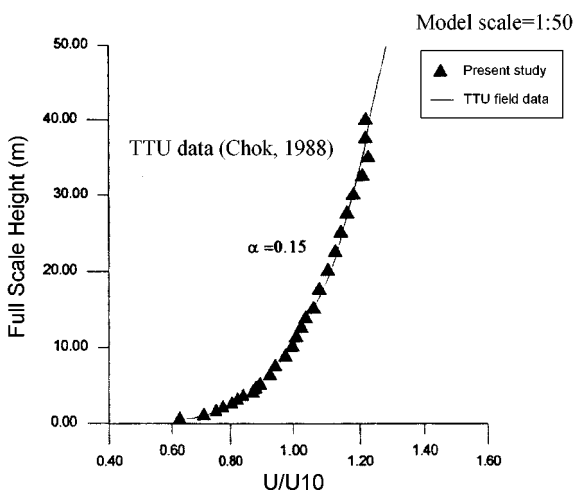


Fig. 3 Mean velocity profile comparison between full scale and model scale

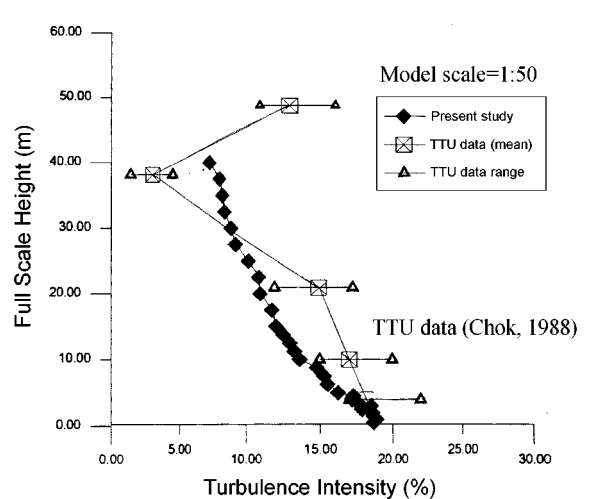


Fig. 4 Turbulence intensity profile comparison between full scale and model scale



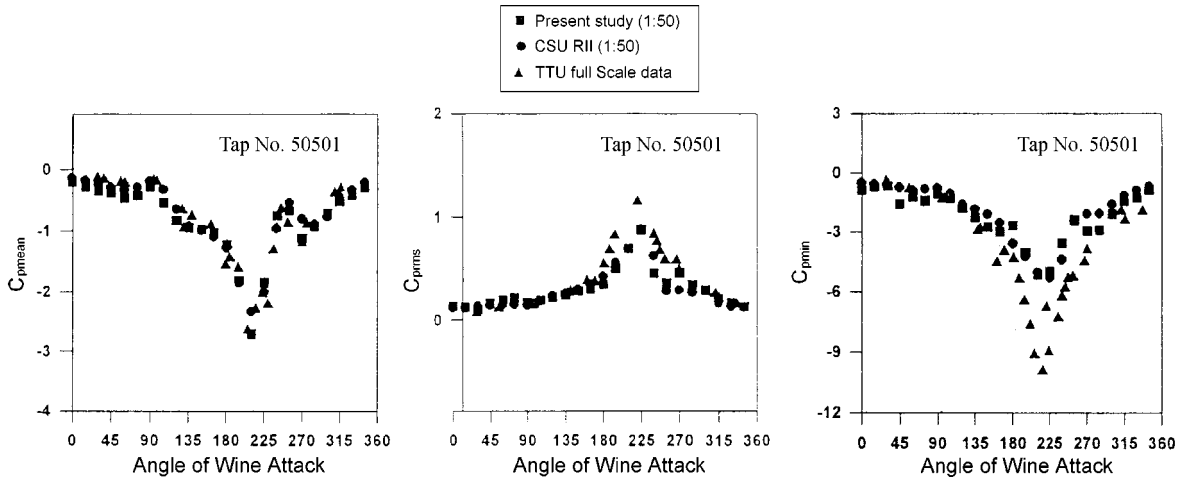


Fig. 6 TTU building  $C_{p\text{mean}}$ ,  $C_{p\text{rms}}$  and  $C_{p\text{min}}$  for roof tap No. 50501

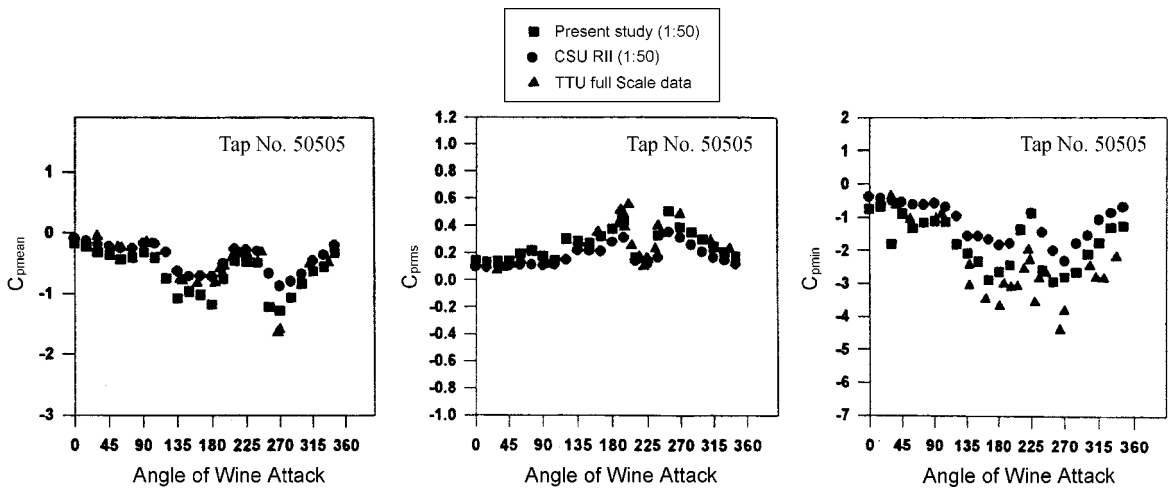


Fig. 7 TTU building  $C_{p\text{mean}}$ ,  $C_{p\text{rms}}$  and  $C_{p\text{min}}$  for roof tap No. 50505

obtained in the test have been compared with CSU RII flow simulated values and TTU full scale values. Values obtained in the present study have been found to be in better agreement with the full-scale values than those of the CSU RII experiment. The  $C_{p\text{min}}$  has also been found to match closely with the full-scale values for wind azimuths between  $180^\circ$  and  $270^\circ$ .

### 2.1.3. Wall tap 42206

The variations of  $C_{p\text{mean}}$ ,  $C_{p\text{rms}}$  and  $C_{p\text{min}}$  with angle of wind incidence are shown in Fig. 8. The values have been compared with the full-scale values and a good agreement with the prototype values has been found.

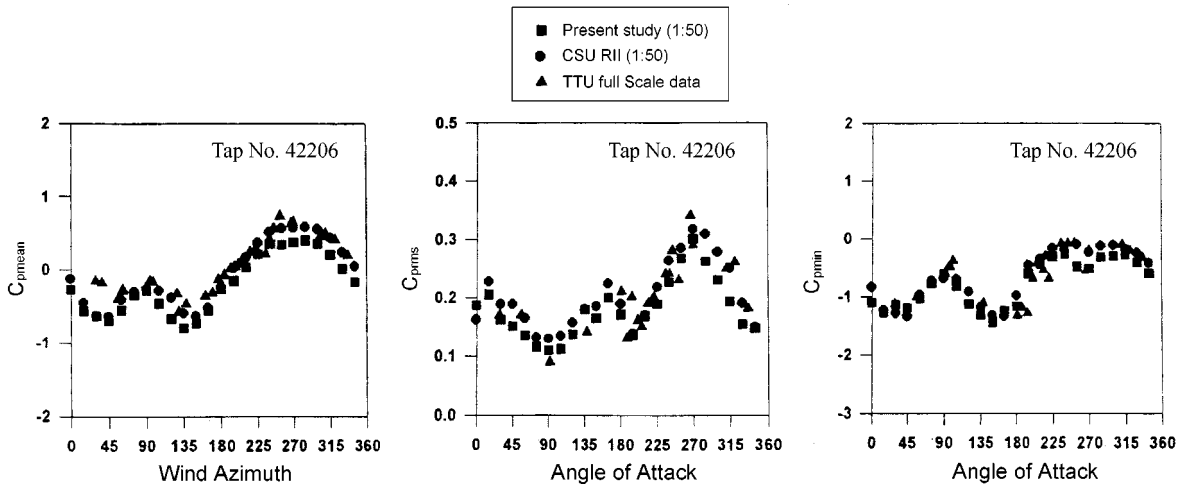


Fig. 8 TTU building  $C_{p\text{mean}}$ ,  $C_{p\text{rms}}$  and  $C_{p\text{min}}$  for wall tap No. 42206

## 2.2. Study of hip roof models

### 2.2.1. Peak pressures

The term ‘peak pressure’ refers to the peak or highest value in a single record of the pressures obtained for a particular wind direction. It has also been related to the mean and rms values by the ‘peak factor’ as follows :

$$\text{Peak pressure} = \text{mean pressure} + \text{peak factor} \times \text{rms pressure}$$

$$\text{Peak suction} = \text{mean pressure} - \text{peak factor} \times \text{rms pressure}$$

The contours for the worst peak suction for all wind directions are shown in Figs. 9 and 10 for each hip roof. For the  $10^\circ$  pitched roof, the hip ridge on the downwind side is the worst loaded region for the hip roof and the largest value of the negative peak pressure coefficient amongst all taps for all wind directions is -4.42. For the  $15^\circ$  pitched roof, the hip ridge on the downwind side is the worst loaded region and the largest negative peak pressure coefficient is -3.35. For the  $20^\circ$  pitch roof, the roof ridge near the hip ridge is the worst loaded region with the largest suction peak coefficient of -3.97. For the  $25^\circ$  pitched roof the roof corner is the worst loaded region and the maximum value of the negative peak pressure coefficient is -4.10 whereas for the  $30^\circ$  pitched roof the worst loaded region is the roof corner and the maximum value of the negative peak pressure coefficient is -4.36. For the  $35^\circ$  &  $40^\circ$  roof slopes of the hip roof the worst loaded region is the windward eave edge near the corner and the largest values of the negative peak pressure coefficient are -4.74 and -4.93 respectively.

The values of  $C_{p\text{peak}}$  (-ve) observed by Xu and Reardon (1998) and the present study for  $15^\circ$ ,  $20^\circ$  and  $30^\circ$  hip roof slopes are given Table 1, which shows similarity in the values.

It is interesting to note that the contour patterns for the worst negative peak suction (irrespective of wind direction) are similar to those of the worst negative mean pressures independent of wind direction. This indicates that the largest magnitudes of the peak pressures are associated with the largest magnitudes of the mean pressures, particularly within the separator bubble region.

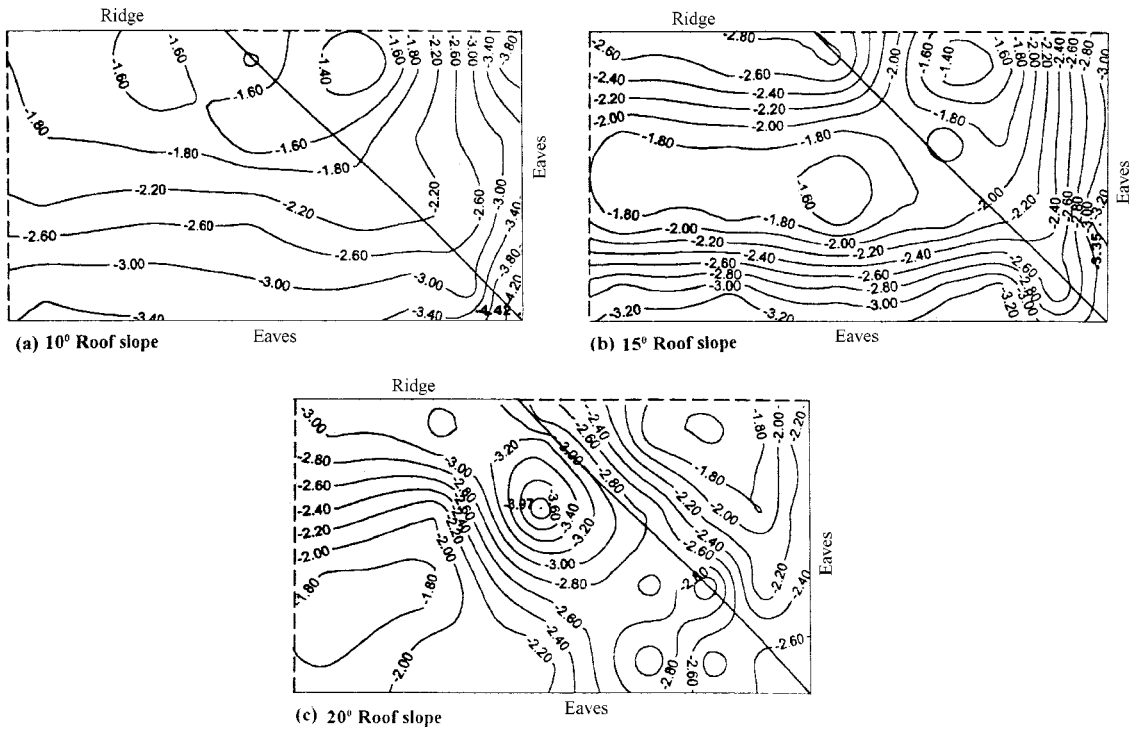


Fig. 9  $C_{pmin}$  for 10°, 15° and 20° roof slope

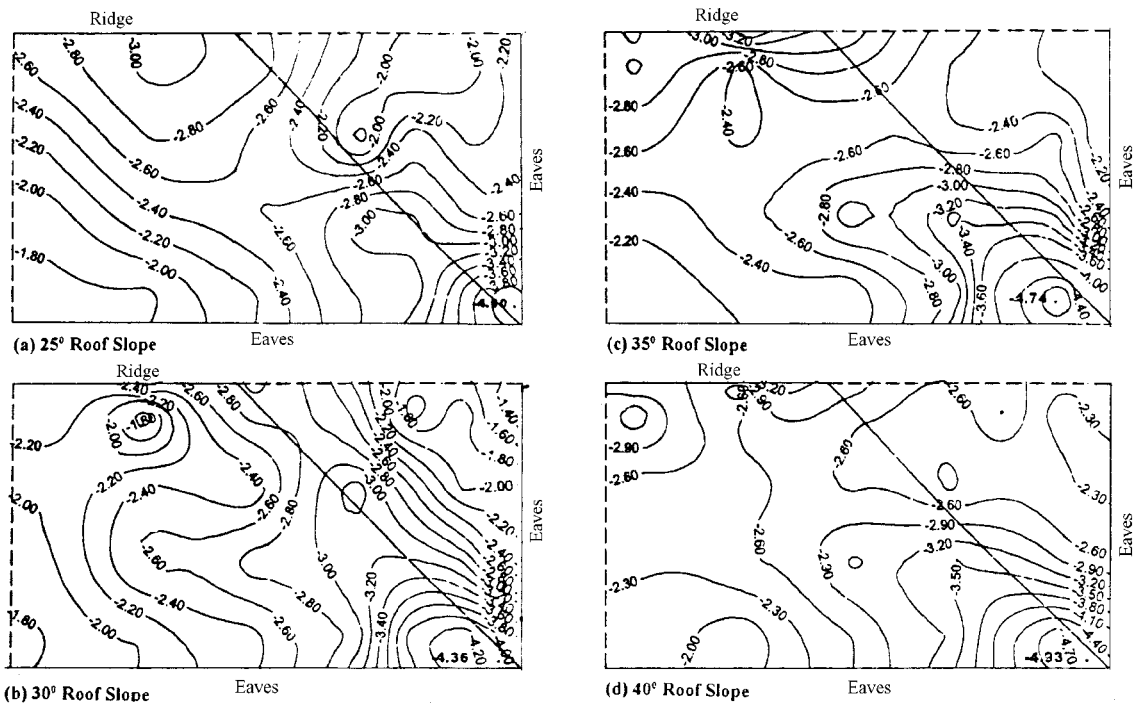


Fig. 10  $C_{pmin}$  for 25°, 30°, 35° and 40° hip roof slope for all wind directions

Table 1 Comparison of maximum values of negative peak pressure coefficients (all azimuths)

Roof Pitch	Xu and Reardon's Work (worst $C_{pmin}$ , all azimuths)	Present Work (worst $C_{pmin}$ , all azimuths)
10°	-	-4.42
15°	-3.5	-3.35
20°	-4.6	-3.97
25°	-	-4.10
30°	-5.0	-4.36
35°	-	-4.74
40°	-	-4.93

### 2.2.2. Comparison with Holmes's work on gable roofs

For the 15° pitch roof, the hip ridge on the downwind side is the worst loaded region with the largest value of the suction peak pressure coefficient, amongst all taps and for all wind directions, as -5.0 for the gable roof but only -3.35 for the hip roof. For the 20° pitched hip roof, the roof ridge near the hip ridge is the worst loaded region while for the gable roof the worst area is at the junction between the roof ridge and the gable end. For this pitch of the roof the largest negative peak pressure coefficient for the gable roof is -7.2, but for the hip roof it is only -3.97. For the 30° pitched roof the worst loaded region is the roof corner for both hip roof and gable roof, the largest negative peak pressure coefficient is -5.0 for gable roof and -4.36 for hip roof (Fig. 11). Thus it can be expected that the hip roof cladding will have better performance than the gable roof cladding during a strong wind.

### 2.2.3. Comparison with Meecham *et al.* work on hip roof

Meecham *et al.* (1991) have reported the results of wind tunnel investigations on wind pressures and forces on a hip roofed building. The geometric scale for the building model was 1:100 with a roof pitch of 18.4° and tested in both open country and suburban terrain. The aspect ratio of the building in plan (length / width) and the eaves height were similar to buildings in this study. However, there were no overhangs in their building model and the sampling frequency and duration have not been reported. The pressure coefficients presented by them have been referred to the mean wind speed at mid-roof height.

Comparing the contours for worst negative peak pressure coefficient (Fig. 12) for 18.4° roof slope (Meecham *et al.*) and the 15° and 20° hip roofs (present study) shown in Fig. 12b and c, one can see that contours patterns for the 15° hip roof from the two sources are similar, but the pressure magnitudes from the present study are lower than those of Meecham *et al.*

### 2.2.4. Design pressure coefficients

Wind pressures on building roofs are highly fluctuating and random in nature. Design pressure coefficients ( $C_{pq}$ ) for any zone of the roof of the building can be deduced from the most critical values of the peak pressures measured in the experiment. The measured peak pressures at a point corresponding to the maximum wind speed, with wind approaching the building from the most

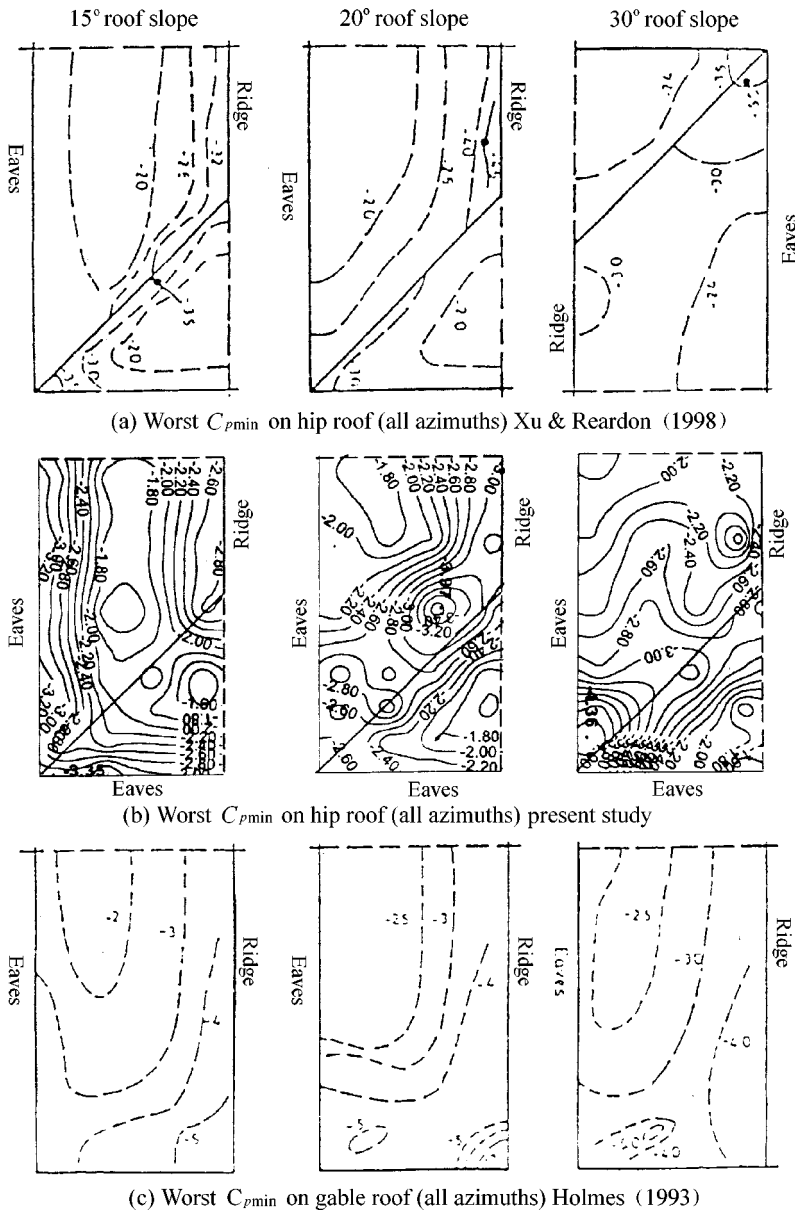
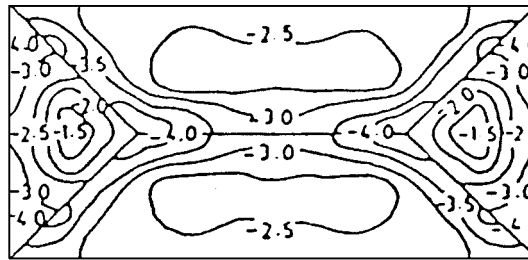
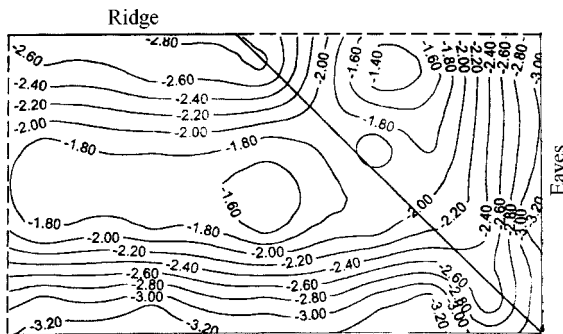


Fig. 11 Comparison of worst peak suction independent of wind direction over 15°, 20° and 30° hip roof slopes

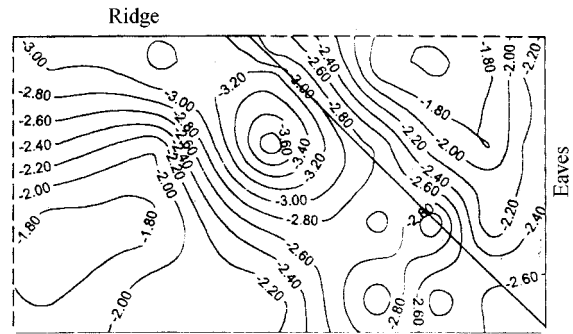
critical direction, are likely to occur only rarely and thus it is more logical to take a reduced value for the design. In the present work, a ‘peak factor’ has been calculated from pressure history record for each tap as **Peak Factor** = {Peak Value/rms Value}. About 1% higher peak factors have been dropped and computed the mean of the rest peak factors. The average value of peak factor obtained here is 3. A simplified procedure given in the BRE Report Digest No. 346, August, 1989 Part-5 has also been used for calculation of gust peak factor ( $g_{Gust}$ ) which is given as :



(a) Worst  $C_{pmin}$  on 18.4° hip roof (all azimuths) Meecham (1991)



(b) Worst  $C_{pmin}$  on 15° hip roof (all azimuths) present study



(c) Worst  $C_{pmin}$  on 20° hip roof (all azimuths) present study

Fig. 12 Comparison of worst negative peak pressure coefficients independent of wind direction on hip roof

$$(g_{Gust})=0.42 I_n (3600/t) \tag{2.1}$$

where  $t$  is the gust duration time in seconds. The gust peak factor obtained from Eq. (2.1) has been shown to be within a few percent of the values obtained from more complex formulations. For the purposes of these procedures, the simplified formula was considered quite adequate. However, it is a factor dependent on the gust duration,  $t$ , which is not of direct interest to the designers. His concern is to choose for static structures, the appropriate gust speed, which will envelop his structure or component to produce the maximum loading.

Fortunately, the bluff type structures, such as buildings, which can be designed statically, there is a simple empirical relationship between the duration,  $t$ , and the size of the structure or element,  $t$ , given by

$$t=4.5 b/U \tag{2.2}$$

where  $U$  is the relevant mean wind speed and  $b$  is the diagonal dimension of the loaded area under consideration. This may be whole building, a single cladding element or any intermediate part.

Taking cladding element for hip roof 7.00 m × 2.90 m, the  $g_{Gust}$  obtained using Eqs. (2.1) & (2.2) is 2.924. This is quite close to peak factor obtained as 3 using time history in the present study.

Therefore, to find the design pressure coefficients peak factor is taken 3. The design pressure coefficients have been defined as:

Design pressure Coefficients=Peak Factor × rms value+mean value (Davenport 1964). Plots of

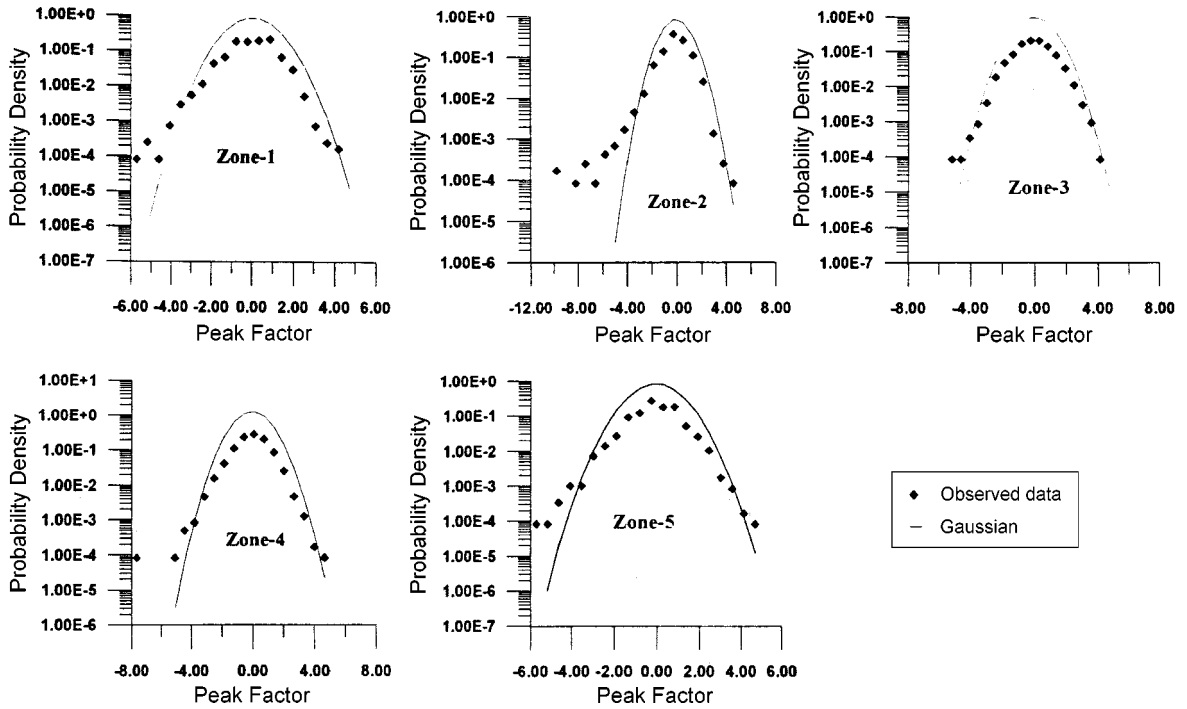


Fig. 13 Plot of probability density functions of pressure fluctuations for Zones 1 to 5 on hip roof

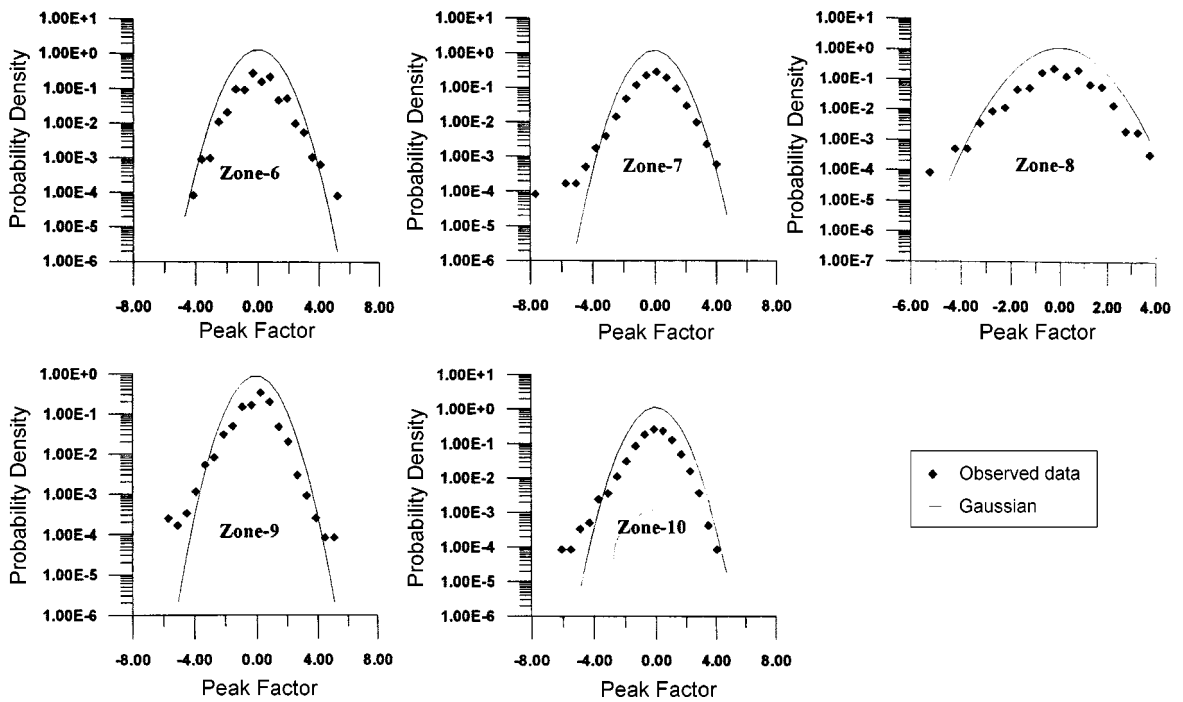


Fig. 14 Plot of probability density functions of pressure fluctuations for Zones 6 to 10 on hip roof

probability density function of the measured pressure fluctuations for different zones over the roof surface have been given in Figs. 13 and 14. These plots show that the observed data follow the Gaussian distribution except for the extremes.

The design pressure coefficients for 10° to 40° roof slopes at an increment of 5° are shown in Figs. 15 and 16. The trend of contour patterns for the design pressure coefficients, irrespective of wind direction, are seen to be similar to those of the maximum rms pressure coefficients. For 10° and 15° roof slopes, the maximum design pressure coefficients are distributed over regions near the corner, along hip ridge and downwind of the hip ridge. As the roof slope increases to 20°, the worst design pressure coefficients occur along the hip ridges and near the junction of hip ridges and roof ridge. For the 25° roof slope, regions near the corner and the area near the roof ridge are observed as heavily loaded area. For the roof slopes of 30°, 35° and 40°, the corner remains the most severely affected region.

### 2.2.5. Critical locations

Variations of the four wind pressure coefficients ( $C_{pmean}$ ,  $C_{pmin}$ ,  $C_{pmax}$  and  $C_{pms}$ ) with the wind angle of incidence have been plotted for the critical taps for the 10° to 40° pitch hip roofs and are shown in Figs. 17 and 18. From these plots, the critical wind directions in which the largest wind

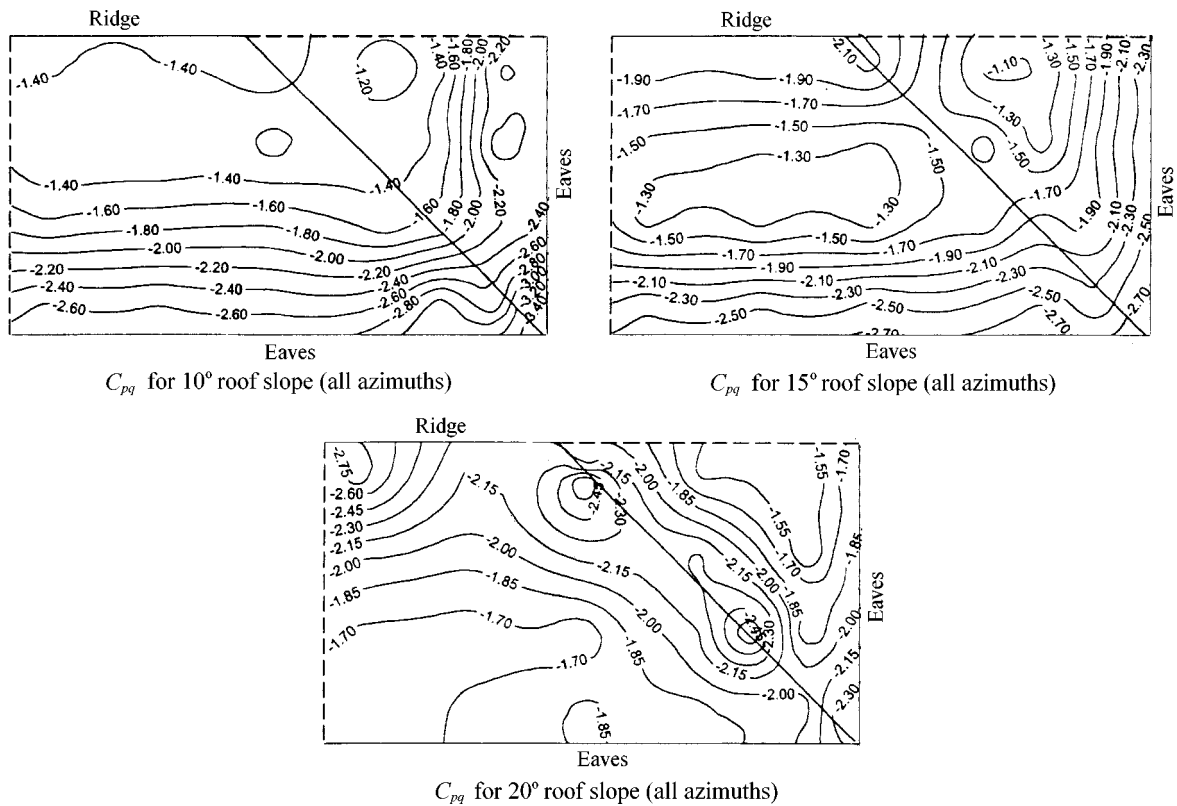


Fig. 15 Design pressure coefficients (Roof slope 10°, 15° and 20°)

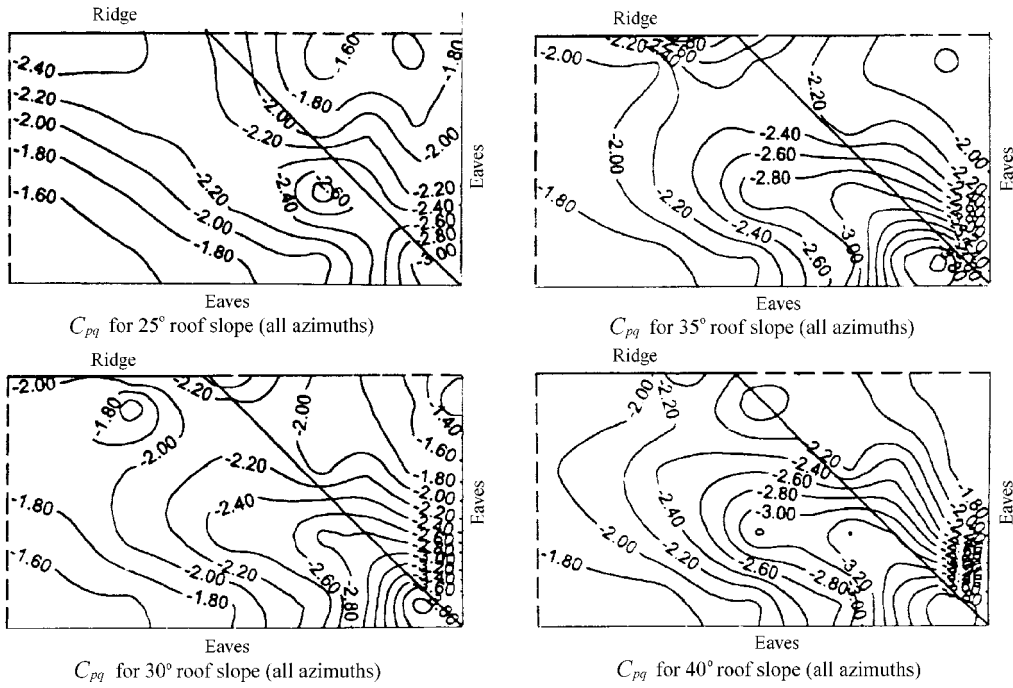


Fig. 16 Design pressure coefficients (roof slope 25°, 30° 35° and 40°)

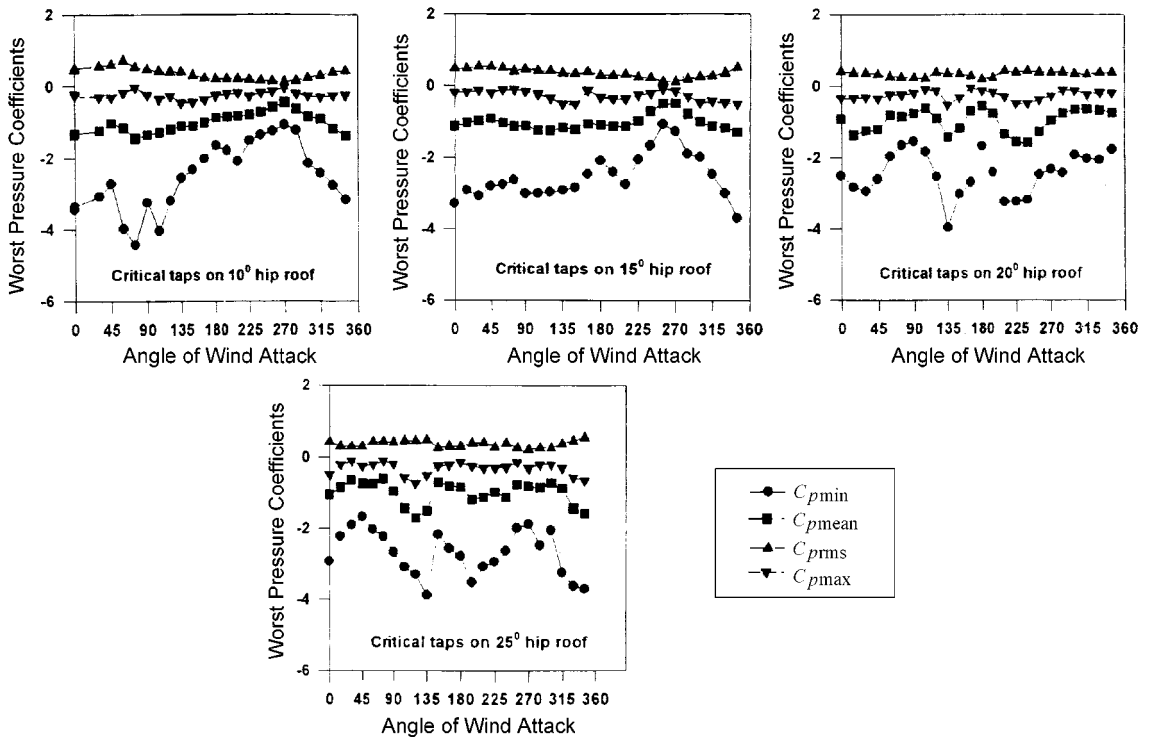


Fig. 17 Variation of pressure coefficients with angle of wind attack on 10°, 15°, 20° and 25° hip roof slopes

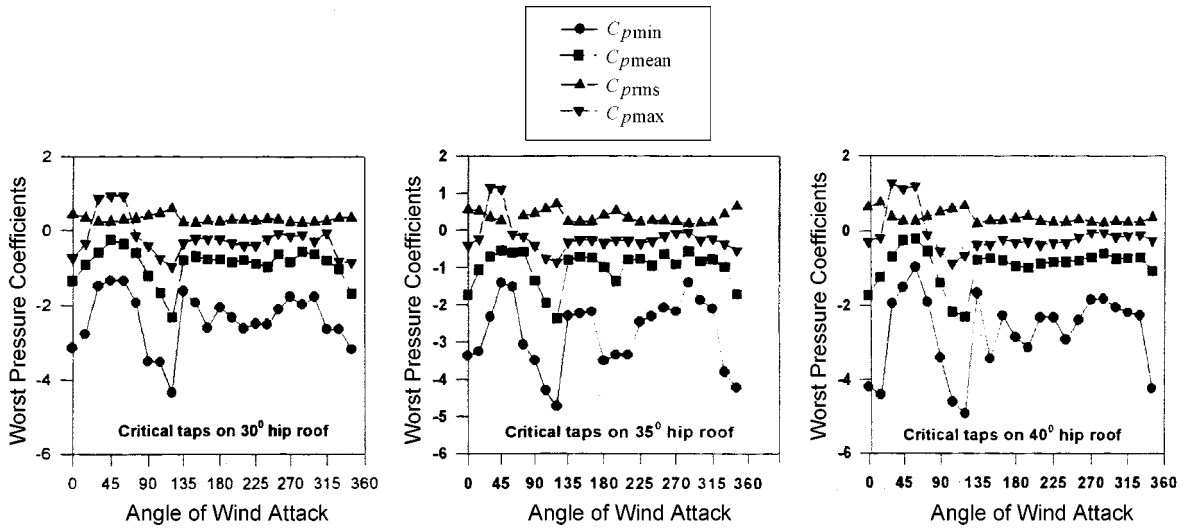


Fig. 18 Variation of pressure coefficients with angle of wind attack on 30°, 35° and 40° hip roof slopes

Table 2 Comparison of critical wind direction for various hip roof slopes

Roof Slope	Critical Wind Direction	
	Xu and Reardon (1998)	Present Study
10°	-	75°
15°	310°	345°
20°	135°	135°
25°	-	135°
30°	120°	120°
35°	-	120°
40°	-	120°

suctions occur can be identified which are given in Table 2. It can also be seen from these plots that the occurrence of the largest peak suction is sensitive to wind direction for the roof pitch in the range 20° to 40°. That is, a change in the wind direction by 5° to 10° from the critical direction causes a significant reduction in the peak suctions.

2.2.6. Zonal pressure coefficients

Due to symmetry of the building about both axes in plan the wind pressure coefficients over one-quarter of the roof only have been plotted. For this purpose the roof has been divided into 10 zones (Fig. 2) based on BRE Report (1989) and the values of  $C_{pmin}$ ,  $C_{pmean}$ ,  $C_{p rms}$ ,  $C_{pmin80}$  (80% of  $C_{pmin}$ ) and  $C_{pq}$  for all the 10 zones against roof pitch have been plotted as shown in Figs. 19 and 20.  $C_{pmin80}$  was used by National building code of Canada, 1980 for design values on low-rise buildings.  $C_{pmin80}$  and  $C_{pq}$  are found comparable. For each zone average of point pressure coefficients have been taken.

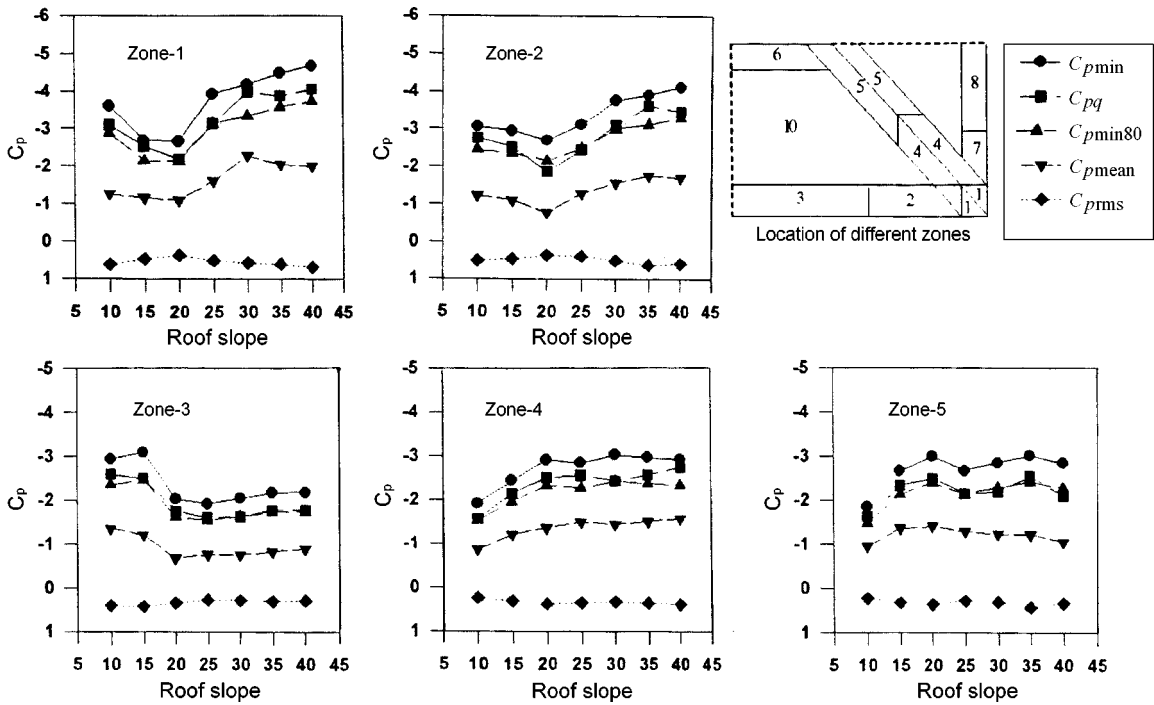


Fig. 19 Variation of pressure coefficients with roof slopes for Zones 1 to 5

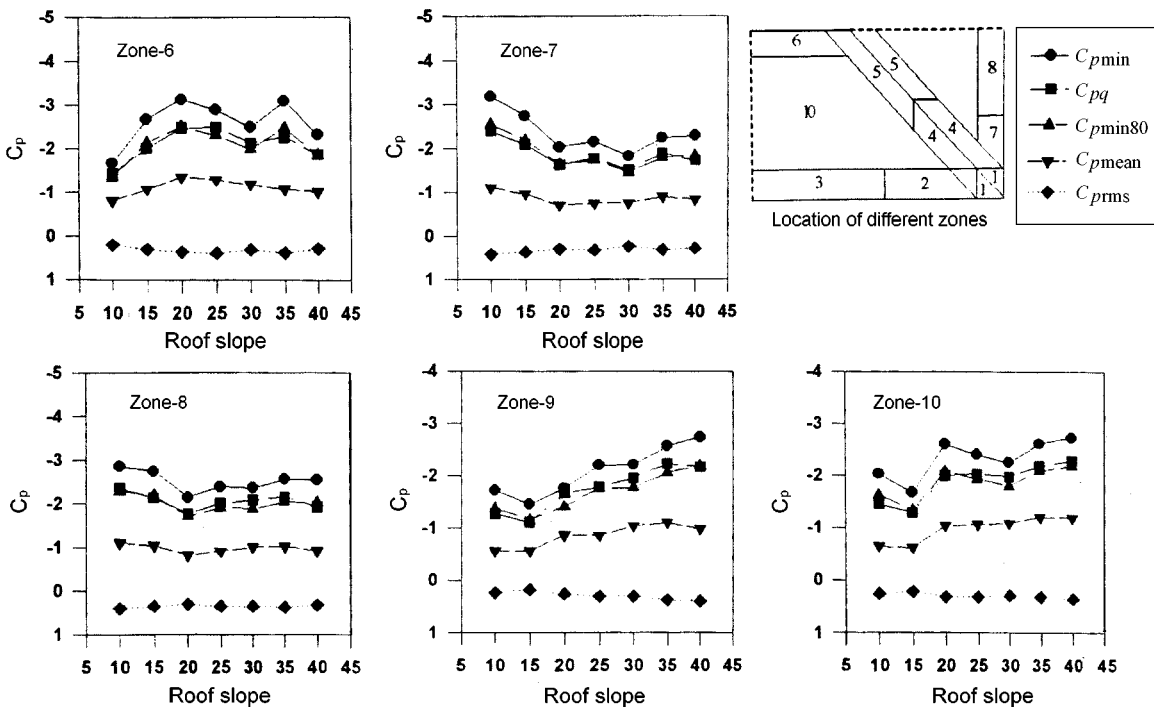


Fig. 20 Variation of pressure coefficients with roof slopes for Zones 6 to 10

Table 3 Pressure coefficients (for mean hourly wind speed) for critical wind directions on various roof slopes

Roof Pitch	Zone	Critical Angle of Wind Incidence	$C_{pmin}$	$C_{pmean}$	$C_{prms}$	$C_{pq}$	$C_{pmin80}$
10°	1	75°	-3.608	-1.268	0.611	-3.101	-2.399
	2	0°	-3.066	-1.250	0.476	-2.679	-2.452
	3	0°	-3.226	-1.363	0.468	-2.766	-2.580
	4	15°	-1.926	-0.539	0.254	-1.436	-1.540
	5	35°	-1.699	-0.906	0.249	-1.652	-1.359
	6	15°	-1.722	-0.835	0.236	-1.542	-1.417
	7	75°	-2.804	-1.021	0.369	-2.211	-2.243
	8	90°	-3.19	-1.029	0.421	-2.294	-2.552
	9	60°	-1.789	-0.481	0.240	-1.201	-1.431
	10	15°	-2.033	-0.602	0.325	-1.576	-1.627
15°	1	75°	-2.710	-1.055	0.502	-2.216	-2.168
	2	15°	-3.016	-1.157	0.474	-2.578	-2.412
	3	15°	-3.279	-1.215	0.412	-2.450	-2.623
	4	45°	-2.337	-1.110	0.292	-1.987	-1.869
	5	45°	-2.686	-1.276	0.318	-2.229	-2.149
	6	45°	-3.775	-0.933	0.265	-1.727	-3.020
	7	75°	-2.755	-0.952	0.371	-2.064	-2.204
	8	75°	-2.807	-0.949	0.386	-2.106	-2.246
	9	60°	-1.315	-0.481	0.193	-1.059	-1.052
	10	15°	-1.684	-0.600	0.245	-1.336	-1.347
20°	1	60°	-2.488	-0.894	0.337	-1.877	-1.991
	2	45°	-2.703	-0.851	0.336	-1.857	-2.163
	3	0°	-1.843	-0.671	0.360	-1.750	-1.475
	4	30°	-2.570	-1.227	0.301	-2.131	-2.056
	5	30°	-2.547	-1.349	0.322	-2.314	-2.037
	6	30°	-3.130	-1.342	0.322	-2.504	-2.504
	7	60°	-2.113	-0.814	0.268	-1.617	-1.690
	8	60°	-2.062	-0.732	0.270	-1.543	-1.650
	9	45°	-2.137	-0.934	0.264	-1.588	-1.709
	10	30°	-2.355	-0.902	0.247	-1.644	-1.884
25°	1	60°	-3.936	-1.535	0.459	-2.912	-3.149
	2	60°	-3.122	-1.242	0.375	-2.366	-2.498
	3	45°	-1.918	-0.755	0.271	-1.569	-1.534
	4	30°	-2.934	-0.975	0.322	-1.943	-2.347
	5	30°	-2.597	-1.027	0.302	-1.934	-2.077
	6	60°	-2.816	-1.178	0.419	-2.436	-2.252
	7	45°	-2.159	-0.748	0.287	-1.609	-1.727
	8	90°	-2.201	-0.751	0.263	-1.539	-1.606
	9	15°	-2.198	-0.856	0.308	-1.781	-1.759
	10	60°	-2.530	-0.857	0.317	-1.807	-2.024
30°	1	60°	-4.190	-2.291	0.566	-3.990	-3.352
	2	60°	-3.758	-1.530	0.491	-3.004	-3.007
	3	60°	-1.974	-0.681	0.296	-1.569	-1.579
	4	60°	-3.021	-1.351	0.261	-2.135	-2.417
	5	15°	-2.847	-0.917	0.276	-1.746	-2.277
	6	60°	-2.442	-1.162	0.305	-2.078	-1.954
	7	30°	-2.293	-0.836	0.294	-1.717	-1.835
	8	45°	-1.812	-0.713	0.239	-1.431	-1.449
	9	15°	-2.313	-1.087	0.286	-1.944	-1.850
	10	60°	-2.437	-1.124	0.306	-2.040	-1.948

Table 3 Continued

Roof Pitch	Zone	Critical Angle of Wind Incidence	$C_{pmin}$	$C_{pmean}$	$C_{prms}$	$C_{pq}$	$C_{pmin80}$
35°	1	60°	-4.485	-2.063	0.604	-3.875	-3.588
	2	75°	-4.193	-1.386	0.547	-3.204	-3.354
	3	60°	-2.031	-0.883	0.323	-1.851	-1.624
	4	75°	-2.955	-1.376	0.323	-2.344	-2.364
	5	15°	-3.013	-1.212	0.440	-2.532	-2.410
	6	75°	-3.078	-0.995	0.293	-2.255	-2.462
	7	30°	-2.323	-0.751	0.264	-1.543	-1.859
	8	30°	-2.142	-0.728	0.229	-1.414	-1.714
	9	15°	-2.368	-1.081	0.337	-2.091	-1.894
	10	75°	-2.451	-1.018	0.331	-2.011	-1.921
40°	1	0°	-4.678	-2.014	0.683	-4.062	-3.742
	2	75°	-4.121	-1.706	0.588	-3.469	-3.297
	3	75°	-2.061	-0.604	0.234	-1.306	-1.649
	4	75°	-2.594	-1.329	0.306	-2.246	-2.075
	5	0°	-2.835	-1.046	0.349	-2.093	-2.268
	6	75°	-2.389	-1.004	0.259	-1.781	-1.912
	7	0°	-2.498	-0.908	0.350	-1.957	-1.998
	8	15°	-2.384	-0.882	0.299	-1.780	-1.907
	9	0°	-2.738	-1.022	0.351	-2.074	-2.190
	10	75°	-2.723	-1.069	0.333	-2.067	-2.178

The critical wind direction for various zones of the roof for various roof pitches has been identified and the same, along with the corresponding values of the pressure coefficients  $C_{pmin}$ ,  $C_{pmean}$ ,  $C_{prms}$ ,  $C_{pmin80}$  and  $C_{pq}$  is given in Table 3.

### 2.2.7. Comparison of design pressure coefficients (3-sec Gust) with building research establishment (BRE) report (U.K.)

A comparison of design pressure coefficients (3-sec gust) of BRE (Building Research Establishment) Report Digest No.346 (Nov.1989) published in U.K., which is compatible with British Standard BS6399 (Part-2), has been made with the results of design pressure coefficients of the present study. The calculated  $C_{pq}$  from  $C_{pmin}$  for hourly mean wind speed has been converted to 3-sec gust as :

$C_{pq}$  (3-sec gust) =  $C_{pmin}$  (hourly mean wind speed)/2.25. A conversion factor of 2.25 is reported in IS875 (part-3).

In the BRE Report, the design pressure coefficients on hip roofs (without overhang) for roof slopes 5°, 15°, 30°, and 45° with wind incidence angles of 0°, 30°, 60°, and 90° have been tabulated. Therefore, comparison for only 15° and 30° hip roof slopes for 0°, 30°, 60°, and 90° wind directions only could be made.

For the 15° roof slope (Figs. 21 and 22), except 0° wind direction, the trends of design wind pressure coefficients are same for 30°, 60° and 90° angles of wind incidence. The design suctions in the present study for the 15° roof slope are lower than in the BRE report for all the zones. For Zones 2, 3, 5 and 9 both the values are closer while for Zones 1, 4 and 6 the values are quite apart. The larger differences are at the corner, along the hip ridge near the corner and the roof ridge zones

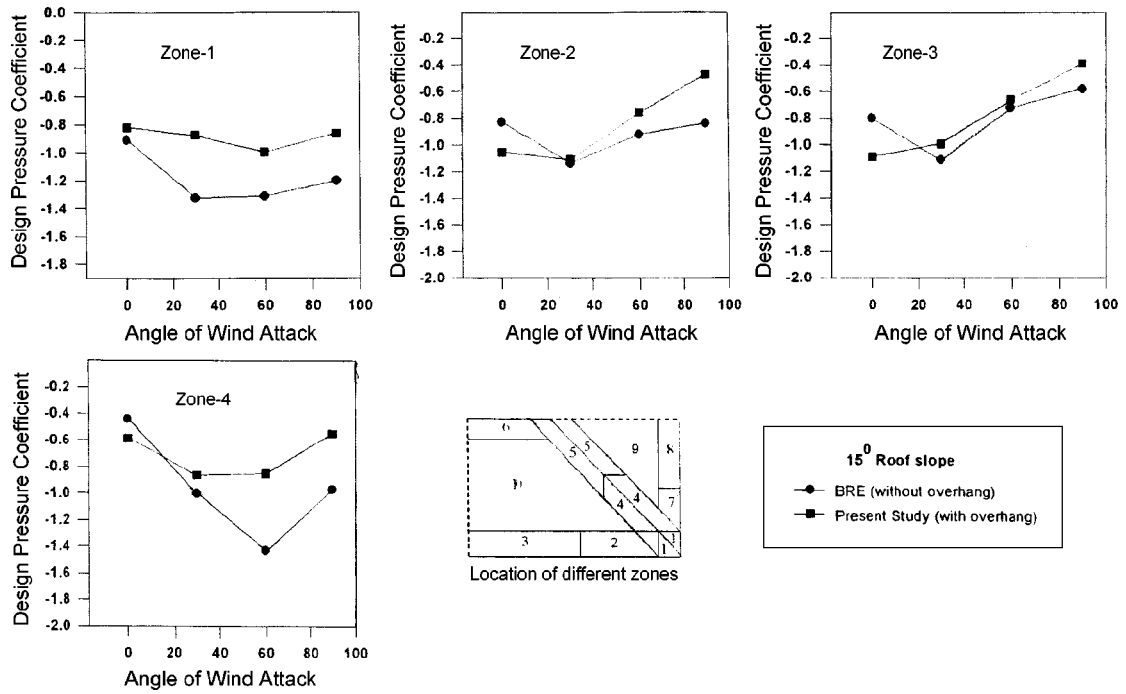


Fig. 21 Comparison of design pressure coefficients (3-sec gust) of BRE report with present study for 15° roof slope for Zones 1 to 4

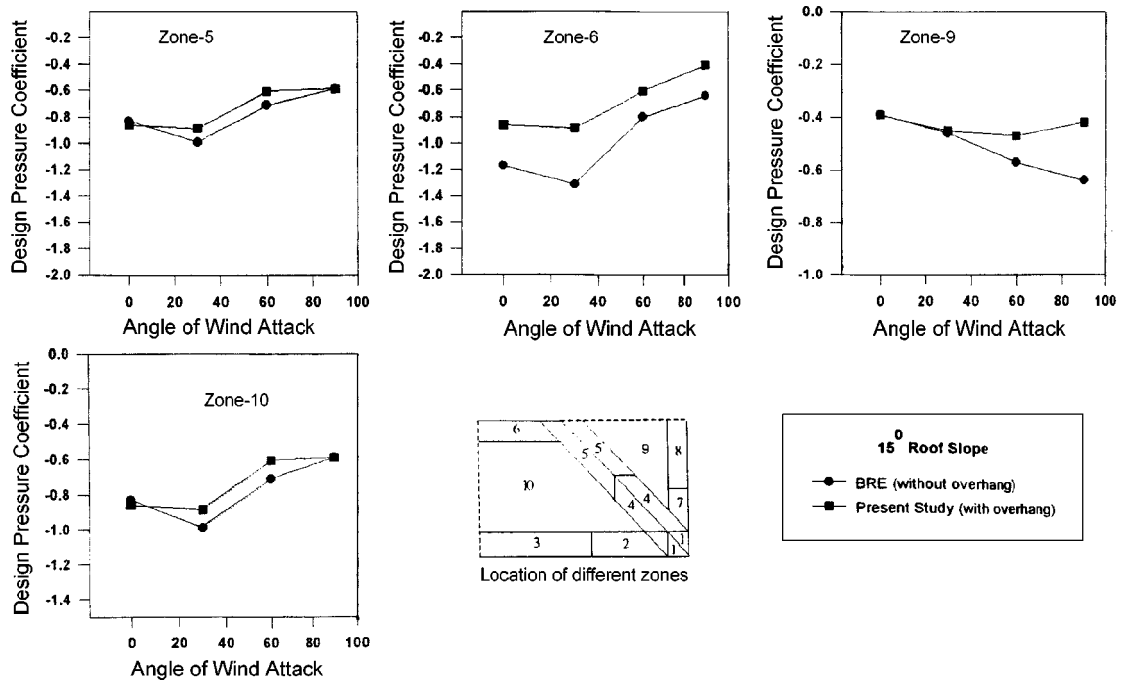


Fig. 22 Comparison of design pressure coefficients (3-sec gust) of BRE report with present study for 15° roof slope for Zones 5, 6, 9 and 10

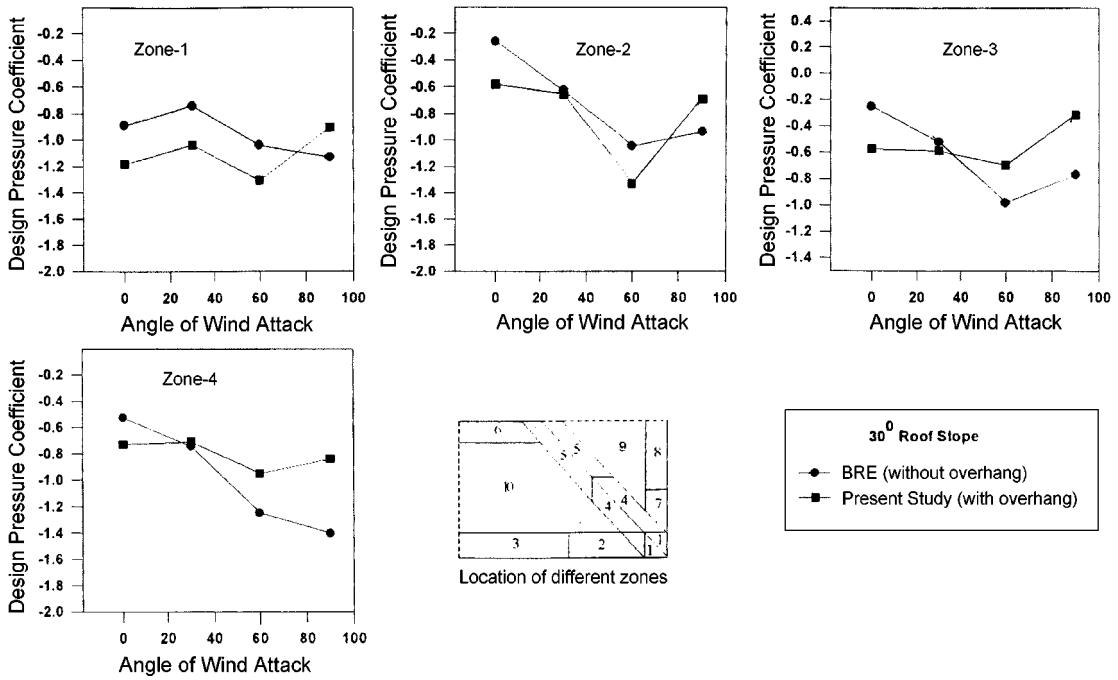


Fig. 23 Comparison of design pressure coefficients (3-sec gust) of BRE report with present study for 30° roof slope for Zones 1 to 4

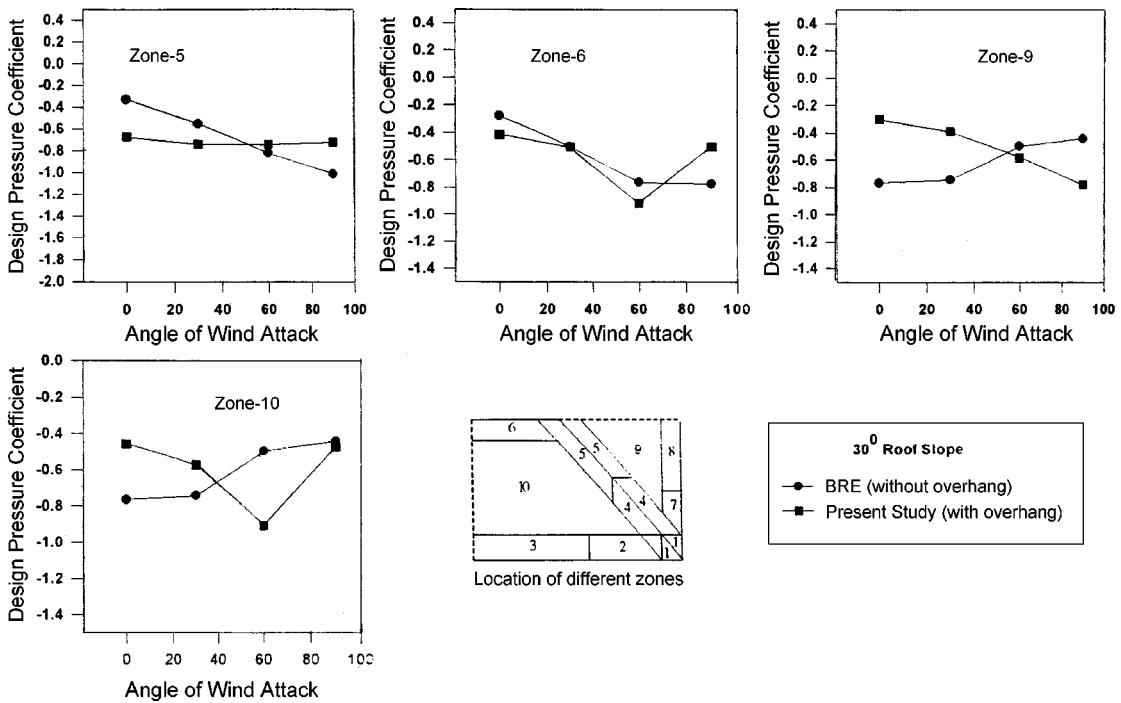


Fig. 24 Comparison of design pressure coefficients (3-sec gust) of BRE report with present study for 30° roof slope for Zones 5, 6, 9 and 10

where separation of the bubble occurs. Also the effect of overhang seems to be significant.

For the 30° hip roof (Figs. 23 and 24), the trend of design suction in Zones 2, 3 and 4 is found to be similar to that in the BRE Report. In Zones 1 and 2, the design suction obtained in the present study are higher than those in the BRE Report. For Zones 3, 4 and 5, upto 30° wind direction, values obtained in the present study are higher but beyond this the values are lower than in the BRE Report. Here also the overhang seems to play a significant role.

### 3. Conclusions

The tests reveal that for the hip roofs the effect of roof pitch on roof pressures is quite significant. An increase in the pitch of a hip roof caused an increase in the worst peak suction. The 40° hip roof experienced the highest peak suction at the roof corner amongst all the seven roofs tested. Compared with the observations of Holmes work on gable roof for 10°, 15°, 20° and 30° pitch, the worst peak suction have been found to be much smaller on the hip roofs for 15° and 20° roof pitch. However, the worst peak suction on the hip and gable roofs were almost the same for roofs having 10° and 30° pitch. It can also be seen that contours for the mean pressure coefficients as well as those for the worst negative peak pressures, irrespective of the wind direction, are compatible with those reported by Meecham *et al.* (1991) and Xu and Reardon (1998). Design pressure coefficients for different zones obtained here are comparable with BRE (1989) Digest No. 346 values although some difference in magnitudes are found. Overhangs may be one of the reasons for such type of difference.

### References

- AS1170.2 (1989), "SAA loading code, Part-2: wind loads, Standard Association of Australia", NSW, Australia.
- BRE Digest (1989), "The assessment of wind loads part 6: loading coefficients for typical buildings", *Building Research Establishment, Department of Environment*, Garsten, WD2 7JR.
- Cochran, L.S. (1992), "Wind tunnel modelling of low-rise structures", Ph.D. Thesis, Colorado State University, USA.
- Davenport, A.G. (1964), "Note on the distribution of the largest value of a random function with application to gust loading".
- Davenport, A.G., Surry, D. and Stathopoulos, T. (1972), "Wind loads on low-rise buildings, final report of phase I and II", *Boundary Layer Wind Tunnel Report BLWT-SS4*, University of Western Ontario, Canada.
- Federal Emergency Management Agency (1992), "Building performance in hurricane Andrew in Florida observations", *Recommendations and Technical Guidance*, Federal Insurance Administration, USA.
- Holmes, J.D. (1994), "Wind pressures on tropical housing", *J. Wind Eng. Ind. Aerod.*, **53**, 105-123.
- IS875 (part-3) 1987, "Indian code of practice for design loads (other than earthquake) for buildings and structures", Bureau of Indian Standards, New Delhi, India.
- Isyumov, N., Fediw, A.A., Colaco, J. and Banavalkar, P.V. (1992), "Performance of a tall building under wind action", *J. Wind Eng. Ind. Aerod.*, **41-44**, 1053-1064.
- Lin, J.X., Surry, D. and Tieleman, H.W. (1995), "The distribution of pressure near roof corners of flat roof low building", *J. Wind Eng. Ind. Aerod.*, **56**, 235-265.
- Meecham, D., Surry, D. and Davenport, A.G. (1991), "The magnitude and distribution of wind induced pressures on hip and gable roofs", *J. Wind Eng. Ind. Aerod.*, **38**, 257-272.
- Okada, H. and Young, C.H. (1992), "Comparison of wind tunnel and full scale pressure measurement tests on Texas Tech. building", *J. Wind Eng. & Ind. Aerod.*, **41-44**, 1601-1612.
- Rofail, A.W. (1995), "Full-scale/model scale comparison of wind pressures on TTU building", *9th International Conference on Wind Engineering*, New Delhi, 1055-1066.

- Sparks, P.R., Baker, J., Belville, J. and Perry, D.C. (1985), "Hurricane Eleva, gulf coast, Aug 29-Sept 2, committee on natural disasters", *Commission on Engineering and Technical Systems*, Natural Research Council, USA.
- Sparks, P.R., Hessig, M.L., Murden, J.A. and Sill, B.L. (1988), "On the failure of single storey wood frame houses in severe storms", *J. Wind Eng. Ind. Aerod.*, **29**, 245-252.
- Tieleman, H.W., Hajj, M.R. and Reinhold, T.A. (1997), "Wind tunnel simulation requirements to assess wind loads on low-rise buildings", *Proc. 2EACWE*, Geneva, Italy, 1093-1100.
- Tieleman, H.W. (1996), "Model/full scale comparison of pressures on the roof of the TTU experimental building", *J. Wind Eng. Ind. Aerod.*, **65**, 133-142.
- Tieleman, H.W., Surry, D. and Mehta, K.C. (1996), "Full/model scale comparison of surface pressures on Texas Tech. experimental building", *J. Wind Eng. Ind. Aerod.*, **61**, 1-23.
- Xu, Y.L. and Reardon, G.F. (1998), "Variation of wind pressures on hip roof with roof pitch", *J. Wind Eng. Ind. Aerod.*, **73**, 267-284.

CC